MOLECULAR ECOLOGY

Long-term in situ persistence of biodiversity in tropical sky-islands revealed by landscape genomics

Journal:	*Molecular Ecology*
Manuscript ID	MEC-17-0387
Manuscript Type:	Original Article
Date Submitted by the Author:	31-Mar-2017
Complete List of Authors:	Mastretta-Yanes, Alicia; CONACYT Research Fellow assigned to CONABIO, Comision Nacional para el Conocimiento y Uso de la Biodiversidad Xue, Alexander; City College and Graduate Center of City University of New York, Department of Biology: Subprogram in Ecology, Evolutionary Biology, and Behavior Moreno-Letelier, Alejandra; Universidad Nacional Autonoma de Mexico, Jardín Botánico, Instituto de Biología Jørgensen, Tove; Aarhus Universitet, Department of Bioscience Alvarez, Nadir; University of Lausanne, Department of Ecology and Evolution Piñero, Daniel; Universidad Nacional Autónoma de México, Departamento de Ecología Evolutiva Emerson, Brent; IPNA-CSIC, Ecology and Evolution;
Keywords:	Transmexican Volcanic Belt, alpine, genetic endemism, ddRAD, aSFS, Comparative phylogeography

Long-term *in situ* persistence of biodiversity in tropical sky-islands revealed by landscape genomics

Alicia Mastretta-Yanes*[1], Alexander T. Xue[2], Alejandra Moreno-Letelier[3], Tove H. Jorgensen[4], Nadir Alvarez[5], Daniel Piñero[6] and Brent C. Emerson[7,8]

1. CONACYT Research Fellow - Comisión Nacional para el Conocimiento y Uso de la Biodiversidad, México, Liga Periférico — Insurgentes Sur, No. 4903, 14010, México, DF, México
2. Biology Department, City College and Graduate Center of City University of New York, New York, NY, 10031, USA.
3. Jardín Botánico, Instituto de Biología, Universidad Nacional Autónoma de México, México, DF, 04510, México
4. Department of Bioscience, Aarhus University, 8000 Aarhus C, Aarhus, Denmark.
5. Department of Ecology and Evolution, Biophore Building, University of Lausanne, 1015 Lausanne, Switzerland
6. Departamento de Ecología Evolutiva, Instituto de Ecología, Universidad Nacional Autónoma de México, México, DF, 04510, México.
7. Island Ecology and Evolution Research Group, Instituto de Productos Naturales y Agrobiología (IPNA-CSIC), C/Astrofísico Francisco Sánchez 3, La Laguna, Tenerife, Canary Islands, 38206, Spain.
8. School of Biological Sciences, University of East Anglia, Norwich Research Park, Norwich NR4 7TJ, UK.

Keywords: aggregate site frequency spectrum, *Juniperus monticola, Berberis alpina*, Trans-Mexican Volcanic Belt, alpine, biodiversity distribution

Corresponding author: Alicia Mastretta-Yanes

email: amastretta@conabio.gob.mx / a.mstt.yanes@gmail.com

Abstract

Tropical mountains are areas of high species richness and endemism. Two historical phenomena may have contributed to this: (1) fragmentation and isolation of habitats have promoted the genetic differentiation of populations and increased the possibility of allopatric divergence and speciation, and; (2) the mountain areas allowed long-term population persistence during global climate fluctuations. These two phenomena have been studied using either species occurrence data or estimating species divergence times. However, only few studies have used intraspecific genetic data to analyse the mechanisms by which endemism may emerge from its most fundamental evolutionary origin: long-term persistence of genetically differentiated populations. Here, we use landscape analysis of genomic SNP data sampled from two high-elevation plant species from an archipelago of tropical sky-islands (the Transmexican Volcanic Belt) to test for population genetic differentiation, synchronous demographic changes and habitat persistence. We show that genetic differentiation can be explained by the degree of glacial habitat connectivity among mountains, and that mountains have facilitated the persistence of populations throughout glacial/interglacial cycles. Our results support the ongoing role of tropical mountains as cradles for biodiversity by uncovering cryptic differentiation and limits to gene flow.

Introduction

Tropical mountains are biodiversity hotspots that tend to have more species than the lowlands surrounding them (Myers *et al.* 2000). Their levels of species richness are particularly high due to the presence of species with wide-ranging distributions and high aggregations of locally endemic species (Kruckeberg & Rabinowitz 1985; Jetz *et al.* 2004). Variation in the contemporary environment may provide some explanation for regional variation in the richness of geographically wide-ranging species, but the high level of endemism present in tropical mountains exceeds predictions using macro-ecological variables alone (Jetz & Rahbek 2002; Rahbek *et al.* 2007). This excess may, however, be explained if analyses incorporate the history of species and their habitats (Jetz *et al.* 2004; Graham *et al.* 2006; Fjeldså *et al.* 2012). Such an integrative approach has suggested that tropical mountains are rich in biodiversity because they promote both species differentiation and long-term population persistence (Fjeldså *et al.* 2012). This represents a new and exciting advance that calls for phylogenetic and phylogeographic data to further our understanding of the origin and maintenance of low-latitude mountain biodiversity.

The small surface area of high mountain regions and their geographic isolation leads to small and fragmented populations. Such a scenario is expected to favour allopatric speciation and hence the evolution of many new endemic taxa (Kessler 2002). Several studies confirm this expectation and it is the most commonly cited explanation for elevational patterns of endemism (Kessler 2002). Parapatric speciation may also occur, although it seems to be a less frequent phenomena (Weir 2009; Cadena *et al.* 2011; Päckert *et al.* 2012). With regard to allowing population persistence through time, tropical

77 mountains have been found to be areas of low climate change velocity, meaning they are
78 areas where biodiversity can survive through periods of global climate fluctuation through
79 small altitudinal shifts instead of long latitudinal movements (Loarie *et al.* 2009; Sandel *et*
80 *al.* 2011). Areas of low climate change velocity thus allow for relatively *in-situ* (within a
81 close horizontal distance to where they exist today) long-term population persistence, in
82 contrast to the range shifts or extinctions that are inferred for higher latitudes and
83 shallower lands (Hewitt 1996; Sandel *et al.* 2011). Population persistence is meaningful for
84 the accumulation of endemism because it leads to the local aggregation of endemic species
85 over time (Fjeldså *et al.* 1999).

86 The allopatric speciation and long-term persistence hypotheses have been examined
87 using species occurrence data (e.g. Sandel *et al.* 2011; Krömer *et al.* 2013) and, more
88 recently, incorporating molecular data for the estimation of species divergence times (e.g.
89 Smith *et al.* 2014). The scale of analysis ranges from coarse continental data (Rahbek *et al.*
90 2007; Sandel *et al.* 2011; Fjeldså *et al.* 2012) to more detailed analyses of specific mountain
91 ranges such as the Andes (e.g. Fjeldså *et al.* 1999; Kessler 2002), the Himalayas (e.g.
92 Päckert *et al.* 2012) and the Eastern Arc Mountains of Tanzania and Kenya (Fjeldså &
93 Bowie 2008). Although these studies have included an evolutionary perspective by jointly
94 analysing species ranges with phylogenetic data, there remains a need for intraspecific
95 analyses of the mechanisms by which endemism may emerge from its most fundamental
96 evolutionary origin: genetic differentiation among populations.

97 We address this knowledge gap by examining population genetic differentiation and
98 habitat persistence within high-altitude tropical mountains, using as a study area the
99 highest mountains of the Trans-Mexican Volcanic Belt (TMVB, Fig. 1). We take a population

level approach because it is expected that areas that facilitate population persistence over intraspecific (phylogeographic) timescales should, in the absence of further geological change, also be stable across interspecific (phylogenetic) timescales, such that regions of genetic endemism will eventually lead to regions of high species diversity (Hugall *et al.* 2002; Carnaval *et al.* 2009). Thus, examining population differentiation and long-term population persistence at the microevolutionary scale can contribute to the evolutionary understanding of tropical mountain biodiversity.

To analyse tropical montane taxa over a timescale consistent with population genetic process, we frame our hypotheses under the expectations of a sky-island dynamic for the TMVB (Toledo 1982; Mastretta-Yanes 2015a). The TMVB is an area that comprises an archipelago of sky-islands at ~19ºN (Mastretta-Yanes *et al.* 2015a) where the highest stratovolcanoes (>3,000 masl) emerged during the last 1.5 Myr (Ferrari *et al.* 2012). Species with current range limits above 3,000 masl are expected to: (1) have been restricted to high-elevation refugia during the interglacial periods of the Pleistocene (such as the present), where divergence could be promoted by restricted gene flow; and (2) have extended ephemerally to lowlands during glacial periods, where the probability of genetic admixture would be increased (Toledo 1982; Mastretta-Yanes 2015a). Therefore, for the TVMB, population differentiation is expected to be a function of topographical variables. Demographically, this sky-island dynamic translates into cycles of population contraction (interglacial periods) and expansions (glacial periods), which should be temporally synchronous among the different mountains, assuming these climatic conditions resulted in a pervasive effect. If glacial-interglacial habitat persistence within mountains that are

122 otherwise isolated from each other occurs over extended periods, populations would also
123 be expected to accumulate private genetic diversity.

124 To test the above-mentioned expectations, we focus on two timberline-alpine
125 grassland plant species of the TMVB for which we generated genomic SNP data, *Juniperus*
126 *monticola* and *Berberis alpina*, and the glacial/interglacial distribution of their habitat type.
127 We first examine the distribution of suitable conditions across sampled mountains through
128 limited altitudinal range changes during glacial/interglacial stages. We then examine if
129 genetic differentiation can be explained by the degree of historical or contemporary habitat
130 connectivity among mountains. Finally, we estimate demographic change across
131 populations within a comparative framework to evaluate how landscape has shaped
132 biodiversity through time. Within our comparative framework, genetic differentiation is
133 expected to correlate with habitat connectivity regardless of intrinsic species
134 characteristics, and demographic changes driven by sky-islands dynamic are thus expected
135 to occur synchronously in both taxa. We then use these data to evaluate the general
136 hypothesis that long-term environmentally stable conditions for these ecosystems
137 persisted *in situ* throughout glacial/interglacial cycles.

138

139 **Methods**

140 *Study system and sampling*

141 *Juniperus monticola* (Cupressaceae) and *Berberis alpina* (Berberidaceae) are shrubs that
142 grow from 3,300 to 4,200 metres above sea level (masl) on rocky formations from above
143 the timberline and into alpine grasslands of the TMVB (Adams 2014; Mastretta-Yanes *et al.*

2014). They are closely related to *J. flaccida* and *B. moranensis*, which grow at lower altitudes (800-2,600 masl and 1,800-3,150 respectively).

Mountain peaks from >3,000 masl within the TMVB and nearby areas of the Altiplano Sur (AS) and the Sierra Madre Oriental (SMOr) were surveyed for *B. alpina* and *J. monticola* during September-October 2010 and April-May 2011 (Fig. 1). *Berberis alpina* was found in a total of six of the 17 locations surveyed, and *J. monticola* in 13, which represent their known distribution within the TMVB and the AS. Samples of the closely related species and outgroups *B. moranensis, B. trifolia, B. pallida, J. flaccida, J. zanonii* and *J. deppeana* were collected at lower elevations (~2,000-3,150 for *Berberis* and ~800-2,500 masl for *Juniperus*) of the TMVB and at northernmost localities of the SMOr and Sierra Madre Occidental (SMOcc) in October 2010 and 2012. Sampling was performed with SEMARNAT permission No. SGPA/DGGFS/712/2896/10. Herbarium specimens of *B. alpina, B. moranensis, J. flaccida* and *J. monticola* were prepared and deposited within the Herbario Nacional in Mexico City (MEXU) or within Herbario CIIDIR in Durango.

Molecular methods

Based on data from related species, the sampled *Berberis* species are likely diploid with an expected genome size of between 0.50 to 1.83 Gbp (Rounsaville and Ranney, 2010), while the *Juniperus* are also likely diploid but with an expected genome size of 9 to 10 Gbp (Zonneveld 2012). For both taxa, ddRAD libraries were prepared using modified versions of protocols by Parchman et al. (2012) and Peterson et al. (2012). For *Berberis*, the enzyme pair EcoRI-HF and MseI was used, while for *Juniperus*, the rare cutter SbfI-HF was used instead of EcoRI-HF, thus allowing for a narrower subsampling of the larger juniper

genome. Samples were randomly divided into three (*Berberis*) or 10 (*Juniperus*) groups with a common sequencing index (ddRAD libraries hereafter). All *Berberis* and two *Juniperus* libraries were sequenced using single-end reads (100 bp long) in a separate lane of an Illumina HiSeq2000, while two libraries were sequenced in a single lane of the same platform for the rest of the *Juniperus* libraries. Further details on *Berberis* laboratory protocol and sequencing output are detailed in Mastretta-Yanes et al. (2015b). For *Juniperus* this information is available in Supporting Information 1.

The *Berberis* dataset consists of 75 individually tagged specimens of *B. alpina* and *B. moranensis* (6-10 per mountain, Table 1), three samples of each outgroup (*B. trifolia* and *B. pallida*) and 15 replicated samples, with at least one replicate per population or species. The *Juniperus* dataset consists of 137 individually tagged specimens of *J. monticola* (10 per mountain, Table 1), four of *J. flaccida,* one of *J. deppeana,* one of *J. zanonii,* 10 negative controls and 20 replicated samples, with at least one replicate per sampling locality or species (with the exception of *J. deppeana*).

Sequencing output, de novo *assembly and loci filtering of RAD data*

Complete details of *Berberis* sequencing output and quality filtering are available in Mastretta-Yanes *et al.* (2015c). Briefly, after demultiplexing and quality trimming of *Berberis* raw reads, final sequences were 84 bp long. *Juniperus* raw reads were demultiplexed and quality filtered using *Stacks* v. 1.17 by: (1) truncating final read length to 87; (2) removing any reads with an uncalled base; (3) discarding reads with low quality scores (score limit 22 to 28, depending on the library); (4) discarding reads that have been marked by Illumina's chastity filter as failing; (5) filtering adapter sequences, and; (6)

rescuing tags (maximum distance of one between barcodes). See Supporting Information 1 for full details on *Juniperus* bioinformatic pipeline.

Here we refer to a RAD-locus as a short DNA sequence produced by clustering together RAD-alleles; in turn, RAD-alleles differ from each other by a small number of SNPs in certain nucleotide positions (SNP-loci). Data were *de novo* assembled using the software *Stacks* (Catchen *et al.* 2011, 2013). Data from *Berberis* had been previously assembled in *Stacks* v. 1.02 with the parameter values *m*=3, *M*=2, *N*=4, *n*=3, *max_locus_stacks*=3 and a SNP calling model with an upper bound of 0.05 (Mastretta-Yanes *et al.* 2015c). Stacks v. 1.17 was used for *Juniperus* with the parameter values *m*=10, *M*=2, *N*=4, *n*=3, *max_locus_stacks*=4 and default SNP calling model. These settings were chosen after testing a wide range of parameters as in Mastretta-Yanes *et al.* (2015c), and optimising the recovery of a large number of loci while reducing the SNP and RAD allele error rates (Supporting Information 1). After *de novo* assembly, the data were filtered to keep only those samples that had more than 50% and 35% of the mean number of loci per sample for *Berberis* and *Juniperus,* respectively (different percentages were used according to sample size), and only those loci present in at least 80% of *Berberis* samples and 70% of *Juniperus*. Putative paralogous loci of the *Berberis* dataset were filtered by identifying loci where the frequency of the major allele equalled p=0.5 in more than one population or species, as detailed in Mastretta-Yanes *et al.* (2014). For the *Juniperus* dataset the same procedure was followed, but with the following modifications in response to the larger sample size: (1) putative paralogous loci had to meet the extra condition of showing the deviations from Hardy-Weinberg Equilibrium (HWE) of H_{obs} >0.9, negative F_{IS} or F_{IS}=1, and (2) putative paralogous loci private to a single population of *J. monticola* were also excluded by

identifying loci where p=0.5 in any single sampling location, present in more than three individuals of that population and showing deviations from HWE. To ameliorate the effect of missing data on population genetics statistics, RAD-loci that were present in several sampling locations but represented by only one individual in any given population were also filtered. These extra conditions were not performed in the *Berberis* dataset due to the small sample sizes for some sampling locations. Replicates were used to estimate error rates for both taxa as in Mastretta-Yanes *et al.* (2015c). For the population genomic analyses, only one sample for each replicate pair was used, along with all the remaining non-replicated samples. For both species, only the first SNP of each RAD-locus was used for population genomic analyses.

Considerably fewer loci were recovered in *Berberis pallida*, compared to the other *Berberis* species, which is likely explained by mutations affecting restriction enzyme cutting sites as a consequence of a distant evolutionary relationship with the other species in the study. This species was therefore excluded from further analyses.

Population genomic statistics and population differentiation

The *populations* program of *Stacks* was used to estimate the number of private alleles, the percentage of polymorphic loci, heterozygosity, π, and F_{IS} at each nucleotide position for each sampling location (mountain) of the ingroup species. Pairwise F_{ST} values were estimated, defining each sampling location as a population. SNP data was exported to PLINK format and analysed with custom R v. 2.15.1 (R. Core Team 2012) scripts.

Timberline-alpine grassland distribution of glacial and interglacial periods

The distribution of the habitat of *J. monticola* and *B. alpina* was modelled using confirmed data points of timberline-alpine grasslands of the TMVB. This "ecosystem approach" to species distribution modeling (SDM) is similar to how Graham *et al.* (2006) modeled rainforest expansion and contraction across climate fluctuations to examine the effect of habitat persistence on rare species occurrence. Although this approach has been shown to perform below average with respect to model sensitivity, it excelled in specificity statistics and robustness against extrapolations far beyond training data, suggesting that the ecosystem approach is well suited to reconstruct historical biogeography and glacial distributions (Roberts & Hamann 2012). Alpine grassland herbarium and fieldwork records were used as presence points and independent environmental variables were extracted from the 19 bioclimatic layers of Hijmans *et al.* (2005). The modeling was performed using Maxent v. 3.3.3k (Phillips *et al.* 2006) and the potential distribution of the timberline-alpine grassland was projected to the LGM using the bioclimatic layers obtained from CCSM and MIROC initiatives (Braconnot *et al.* 2007). Full details of the modelling are available in Supporting Information 2.

Landscape genomics analyses

To examine if genetic differentiation and endemism can be explained by the degree of historical spatial isolation among mountains we tested for isolation by resistance (IBR) *vs* isolation by distance (IBD). The approach is similar to studies where the influence of landscape features on population structure is investigated (e.g. McRae *et al.* 2008; Moore *et al.* 2011).

Resistance distances (McRae 2006) for the IBR tests were used to estimate the effective distance among sampling localities, using as conductance grid (the reciprocal of the resistance) each of the 13 resistance surfaces described below. This method is based on circuit theory and considers multiple potential paths of least resistance between sampling points (McRae 2006), thus performing better than similar approaches like least-cost path analysis (McRae & Beier 2007; Moore et al. 2011). Mantel tests with 10,000 permutations were performed to test for IBR and IBD using the pairwise effective distances for each resistance surface and the pairwise F_{ST} matrices of genetic differentiation for each species. For this, the genetic differentiation matrices were linearized using the formula for isolation by distance F_{ST} /(1 – F_{ST}) as advocated by Rousset (1997). Subsequently, partial Mantel tests with 1,000 permutations were performed partialling out the flat resistance distances. Tests were carried out independently for both species and also for a subset of *J. monticola* populations (excluding Nevado de Colima and Tancítaro, see discussion for reasons). Analyses and graphical representations of data were performed with R using the packages *ape* (Paradis *et al.* 2004), *vegan* (Oksanen *et al* 2016), *ade4* (Dray & Dufour, 2007) and *ggplot2* (Wickham & Chang 2013).

The 13 resistance surfaces used here were based on: (i) environmental modelling ("present", "CCSM" and "MIROC" for the LGM); (ii) a "flat" landscape, and; (iii) elevation data (above 1800, 2000, 2300, 2500, 2700, 3000, 3300, 3500 and 4000 masl; Fig. 2). The 'flat' landscape surface is equivalent to testing for IBD using Euclidean distances, but it takes into account the fact that the underlying landscape is bounded and not infinite (Lee-Yaw *et al.* 2009; Moore *et al.* 2011). Resistance distances were estimated using the pairwise mode of the program *Circuitscape* v. 3.5.8 (McRae 2006; McRae & Beier 2007) setting the

sampling locations as focal points. For further details on generating the resistance distances see Supporting Information 2. The average effective distance of each sampling locality to the rest of the sampling localities was estimated from a pairwise distance matrix.

Comparative demographic inference using the aggregate site frequency spectrum

We tested which demographic syndrome (population expansion, contraction or constant size) best fits the history of each sampled mountain locality for both species, and we then examined if the inferred demographic changes were synchronous. To accomplish inference of synchronicity, we used a recently developed method that allows for comparative demographic inference of independent, co-distributed taxa, species and populations within a unified analysis (Xue & Hickerson, in revision; Xue & Hickerson, 2015, and see Prates *et al* 2016 for an applied example). The method exploits the aggregate site frequency spectrum (aSFS), which is a summary statistic vector that contains signal of co-demography. The aSFS is assembled via a re-ordering procedure applied to genomic-scale data in the form of the site frequency spectrum (SFS) across independent populations (either simulated or empirical). This is then coupled with an inferential framework to compare observed and simulated aSFS data under a hierarchical co-demographic model that freely hyperparameterizes degree of synchronicity (Xue & Hickerson, under review). Three main steps were followed to perform this analysis:

a. Downprojecting SNP data to equal sampling size. Since the aSFS assumes independence among populations, we re-performed SNP calling on each population individually in order to maximize the number of SNPs while also minimizing the amount of missing data within each population. The aSFS requires all populations to be sampled for

the same number of individuals, with simulations requiring the same number of SNPs for each population. A trade-off thus exists between higher number of individuals and less populations with an adequate number of SNPs (at least 600, usually around 1,000) due to missing data causing a large reduction of SNPs. To address this, two downprojected datasets were constructed, allowing for differing in the number of individuals per population. This was achieved by running the *populations* program of Stacks to export SNPs to keep loci that were present in a minimum of 4 and 5 individuals per population (*-r* flag), respectively. The SNP data of each population were then downprojected using *dadi* 1.7 (Gutenkunst *et al.* 2009) to an SFS with sampling sizes of 4 and 5 respectively.

b. Independent single population demographic analyses. First *fastsimcoal* version 2.5 (Excoffier *et al.* 2013) with the FREQ setting was used to directly generate 100,000 folded SFS simulations per model of instantaneous expansion, instantaneous contraction, and constant size for a total of 300,000 simulations, per each of the two downprojection datasets. Each SFS was simulated under 1,000 genealogies, which is based on the average number of SNPs across all the empirical SFS, and the following priors: time of size change $\tau \sim U\{1{,}000, 250{,}000\}$ generations ago; magnitude of size change $\varepsilon \sim U(0.02, 0.20)$ for expansion model and $\sim 1/U(0.02, 0.20)$ for contraction model; effective population size $N_e \sim U\{100{,}000, 2{,}000{,}000\}$ for expansion model, $\sim U\{50{,}000, 500{,}000\}$ for constant size model and $\sim U\{5{,}000, 100{,}000\}$ for contraction model. Then, to infer demographic syndrome as well as to estimate posterior distributions for time, magnitude of population size change and effective population size, an approximate Bayesian computation (ABC) was done using the R package *abc* (Csilléry *et al.* 2012). Simple rejection was performed with a tolerance level of 0.005.

c. Comparative co-demographic aSFS-based analysis. The results of the single population analyses were used to inform the multi-population synchronicity analysis. As a result there were 10 expanders and four contractors (total of n = 14 populations) for the data downprojected to four individuals, and eight expanders and four contractors (total of n = 12 populations) for the data downprojected to five individuals. The priors for the SFS simulation were set to : time of size change ~ U\{100,000, 2,000,000\} generations ago with a pulse buffer on the prior β = 20,000 generations (forcing all other time draws to be > 20,000 generations apart from each synchronous pulse timing; Xue & Hickerson, in revision), magnitude of size change ~ U(0.05, 0.20) for expansion model and ~ $1/U$(0.05, 0.20) for contraction model, and effective population size ~ U\{50,000, 500,000\} for expansion model and ~ U\{5,000, 100,000\} for contraction model. Per dataset (downprojections to four and five individuals), two reference tables were constructed, each with a different hyperparameterization scheme. Following Xue & Hickerson, (in revision) the two hyperparameterization schemes included: 1) restricting synchrony to only a single pulse and varying the proportion of taxa having membership within this pulse ζ ~ U\{1, n\}/n, with the remaining taxa temporally idiosyncratic in size change (the case of ζ = 1/n would represent total idiosyncrasy); 2) distributing taxa equally across synchronous pulses, the number of which is varied ψ ~ U\{0, 3\}, thus allowing no idiosyncratic taxa except in the case of total idiosyncrasy (ψ = 0). To clarify, for the latter scenario, when n is not divisible by the number of pulses, the remainder is distributed randomly across as many pulses as possible (*e.g.* if n = 14 and ψ = 3, then a random two of the three pulses would have five taxa and the remaining would have four taxa). To construct each of the four total reference tables, 1,000,000 folded aSFS were simulated, with each aSFS

partitioned between the expanders and contractors such that the SFS simulated under expansion and the SFS simulated under contraction were each separately converted to two aSFS vectors, which were then concatenated (Prates et al. 2016; Xue & Hickerson, under review). Each per-population SFS was simulated under 1000 genealogies using the priors mentioned before.

Hierarchical Random Forest (hRF) was performed for each reference table using the R package *randomForest* (Liaw & Wiener, 2002) and hierarchical ABC (hABC) was performed using the R package *abc* (Csilléry *et al.* 2012). To conduct hRF, we used 100 iterations of randomly selecting 5,000 simulations from the reference table to produce 10 decision trees, with the default 33% of variables per decision tree node. Decision trees were built to capture variation in ζ for the first hyperparameterization scheme and ψ for the second hyperparameterization scheme, and exploited for prediction of respective hyperparameter values from the empirical data using the R function *predict()*. To conduct hABC, simple rejection was performed with a tolerance level of 0.0015. The function *abc()* was deployed for hyperparameter estimation and parameter summary estimation of dispersion index (variance/mean) Ω and mean for timings of demographic changes across populations (with lower values signaling greater synchronicity). Median and mode statistics of posterior distributions were calculated for point estimates. For both hRF and hABC, "leave-one-out" cross-validation, which involves removing a simulation and treating it as a pseudo-observed dataset (POD) for estimation against the remaining reference table, was performed using the function *cv4abc* following the same specifications with 50 total PODs per reference table. Estimated values were leveraged against true POD values to calculate Pearson's correlation *r* and root mean squared error.

Although it is computationally possible to use the aSFS to estimate the timing of demographic events within populations (Xue & Hickerson, under review), both *B. alpina* and *J. monticola* violate key biological assumptions that compromise such estimations, specifically a reproductive system of overlapping generations coupled with long lived reproductive individuals (Peterson 2003; Francis 2004; Adams 2008; Bonner 2008). While these features are not expected to greatly affect inference of co-demography (Xue & Hickerson, under review), they are likely to confound the estimation of timing. This could be addressed by translating number of generations into time by weighing individuals by their reproductive value (Felsenstein 1971), but this is not feasible for our species. While we do not estimate absolute timing, relative timing is assumed to be consistent between populations to test for synchronicity.

Results

Alpine grassland distribution during glacial/interglacial stages

The uncorrelated environmental variables selected for the timberline-alpine grassland modelling were isothermality, mean temperature annual range, temperature in the wettest quarter, precipitation seasonality and precipitation in the coldest quarter (Fig. 3a). For the present conditions (Fig. 3b), our modelling is congruent with the known distribution of the timberline-alpine grasslands in this region (Rzedowski 1978; Calderón de Rzedowski & Rzedowski 2005), but it may represent a slight overestimate (Supporting Information 2 for discussion). The projection to the LGM shows that this ecosystem occurred in the same geographic areas, but with a larger distribution extending to lower elevations (Fig. 3b).

RAD-seq data yield and population genetic statistics

Berberis data used here correspond to the subset of "putative orthologs within *B. alpina*" described in Mastretta-Yanes *et al.* (2014). The dataset contains 3,669 SNPs (considering only the first SNP of each RAD-locus) with an error rate of 2.3% (SD 0.27), 19% missing data and a mean coverage of 10.3 (SD 4.6). For the *Juniperus* data (only *J. monticola* ingroup), 2,925 SNPs (considering only the first SNP of each RAD-locus) were recovered, with a SNP error rate of 1.4% (SD 0.8) and 16% of missing data.

Populations from both species show private alleles ranging 154-1101 and an average nucleotide diversity ranging π=0.08-0.13 (Table 1). The F_{IS} decreases East-West for *Berberis* and shows no clear pattern in *Juniperus*, with values ranging F_{IS} = 0.03-0.07 (Table 1). Pairwise F_{ST} values for *B. alpina* populations ranged from 0.056 to 0.123 and were significant, with the Cofre de Perote population showing the highest levels of differentiation and Tlaloc the smallest (Table S2.1). For *J. monticola* F_{ST} ranged from 0.022 to 0.074 and were significant, with La Malinche population showing the highest values of differentiation and Tlaloc the smallest (Table S2.2).

Isolation by resistance

The plots of the resistance surfaces show that although most sampling points are separated by comparable horizontal distances, there are important differences regarding the connectivity among points, and these depend upon the elevation or distribution model used to set the conductance values (Fig. 2).

418 The Mantel and partial Mantel tests yielded positive significant results with
419 different explanatory power depending on the surface used. The 'flat' landscape (i.e. IBD)
420 was outperformed by some of the scenarios considering the environmental modelling or
421 the elevation grids (Table 2). For *B. alpina* the highest explanatory power was provided by
422 the resistance surface of 3,000 masl both for the Mantel (r = 0.940, p < 0.01; Table 2), and
423 the partial Mantel test (r = 0.717, p < 0.05). For *J. monticola,* considering all populations, the
424 surface with the highest explanatory power was the flat surface (Mantel r = 0.499, p < 0.05)
425 and no partial Mantel test was significant. However, when excluding the populations of
426 Nevado de Colima and Tancítaro, environmental modelling for the LGM using the CCSM
427 layers provided the highest explanatory power both for the Mantel (r = 0.686, p < 0.001)
428 and partial Mantel test (r = 0.453, p < 0.01).
429
430 *Comparative demographic inference*s using the *aggregate site frequency spectrum*
431 A high degree of temporal synchrony among population size changes in both species was
432 detected across both single population and multi-population analyses and both sampling
433 levels. The single population analyses (Table S2.2) showed that 10 populations are
434 consistent with population expansion (*Berberis* Aj, Iz, Ma, TI, *Juniperus* Aj, Bl, Ch, Iz, Ne, Tl;
435 population codes as in Fig. 1, see Supplementary Materials 2 for details on each population
436 inference), four are consistent with contraction (*Berberis* To, *Juniperus* Co, Ma, To), two are
437 consistent with constant size (*Juniperus* Ta, *Berberis* Pe) and two are inconclusive though
438 largely consistent with constant size (*Juniperus* Ci, Pp). The estimates of *N*e seem relatively
439 consistent across populations, mostly ranging from 150-250K for expanders and 50-100K
440 for contractors. The magnitudes (ancient/present population size) were moderate and

441 relatively similar across population expansions (8.2-8.7, given that the factor of expansion
442 is the inverse of expansion magnitude; Table S2.3), whereas the two population
443 contractions exhibited stronger magnitude and increased variability (12.5-14.6, Table
444 S2.3). The single-population and the multi-population aSFS-based analyses are largely
445 consistent with high synchronicity for both the four (Table 3, Tabla S2.5) and five
446 individual (Table S2.4, Tabla S2.5) downprojections.
447
448 **Discussion**
449 We tested for population genetic differentiation and habitat persistence within the TMVB
450 by coupling species distribution modelling for glacial/interglacial cycles, landscape
451 genomic analyses with explicit quantitative hypotheses**,** and analyses of demographic
452 history within a comparative framework. Results support the hypothesis that tropical
453 mountains have facilitated the differentiation and long-term *in situ* persistence of alpine-
454 grasslands species from the TVMB.
455
456 *Altitudinal changes of alpine grasslands*
457 Ecosystem distribution modelling reveals that the alpine grasslands shifted altitude during
458 the Pleistocene climate fluctuations, but would have persisted within some mountains
459 during both glacial and interglacial periods (Fig. 3). It is important to note that both our
460 modelling approach and the available palynological and geological data are not species
461 specific, and taxa may respond differently to subtle environmental differences or have
462 different tolerance thresholds (Araújo & Guisan 2006; Roberts & Hamann 2012).
463 Nonetheless, broadly speaking, the present and past distributions of timberline-alpine taxa

464 from the TMVB are highly dependent on temperature or temperature associated variables,
465 which in turn are highly correlated to altitude (Beaman 1962; Lauer 1978; Almeida-Leñero,
466 *et al.* 2007). Thus, it is expected that the altitude of the landscape separating the highest
467 peaks of the TMVB would play a key role on population isolation.

468 The modelled lower elevations of TMVB timberline-alpine grasslands during the
469 LGM (Fig. 3c) is congruent with fossil pollen records down to 2,300-2,500 masl for reduced
470 forests (similar to open forests close to the timberline) and grasslands (Lozano-García &
471 Ortega-Guerrero 1994, 1998; Lozano-García *et al.* 2005; Caballero-Rodríguez et al. 2017).
472 Moraines also reveal that snow lines dropped by approximately 1,000 m during glacial
473 periods (Lozano-García & Vázquez-Selem 2005; Vázquez-Selem & Heine 2011). Considered
474 together, the palynological, geological and niche modelling data all suggest that open
475 forests and grasslands could have extended down to 2,300-2,500 masl at the LGM, and that
476 suitable conditions for alpine vegetation (now at around 4,000 masl) could have been
477 present at 3,000-3,300 masl.

478 Within the higher stratovolcanoes that reach more than 3,500 masl, altitudinal
479 shifts of approximately 1,000 m can be achieved within a relatively short horizontal
480 distance (3-6 km). This means that the alpine grasslands will shift altitudinally during
481 glacial and interglacial periods, but with only limited horizontal displacement in the
482 highest mountains. When such mountains are flanked by lower altitude terrains, forests are
483 expected to both remain isolated and persistent locally over timescales exceeding the
484 periodicity of a glacial cycle (Fig. 3b-c).

485

486 *Glacial distribution explains population differentiation*

Testing for IBR using surfaces that consider present and past potential habitat distributions shows that, as predicted, accounting for topography-driven connectivity better explains population differentiation than simple geographic distance (Table 2). The population genetic differentiation of both species was better explained by resistance surfaces likely representing their glacial distributions (~1,000 m below the elevation where they are currently more abundant). This result is not surprising when considering that: (1) the timberline attained its present altitude only 3,000 yr ago (Lozano-García & Vázquez-Selem 2005); (2) the last 700,000 yr have been dominated by major glacial periods with a ~100,000 yr cycle interrupted by relatively short warm interglacials (Webb & Bartlein 1992); so that (3) recent distributions could be considered a perturbation of the "historical average", and (4) that *Berberis* and *Juniperus* are slow growing and live for decades and hundreds of years, respectively (Francis 2004; Adams 2008), such that the number of generations representing the present distribution could be relatively small.

For *B. alpina,* the explanatory power was highest in the IBR test with the surface allowing for connectivity at 3,000 masl both in the Mantel test (r = 0.940) and the partial Mantel test (r = 0.717, $p < 0.05$). This indicates that although simple geographic distance provides explanatory power, more of the variance is explained if connectivity through time is considered (Fig. 4). This also holds for *J. monticola*, when Nevado de Colima and Tancítaro populations were excluded from the analysis (Fig. 5), as the IBR test with the LGM-CCSM surface held more explanatory power (Mantel r = 0.686, $p < 0.001$, and partial Mantel r = 0.452, $p < 0.01$; Table 2) than the other surfaces. The Nevado de Colima and Tancítaro mountains are considerably further away from the remaining high mountains of the TMVB (Fig. 1). Importantly however, our models infer that they were not connected by

alpine grasslands to the Central TMVB during the Pleistocene glaciations. They remained isolated in both LGM models, even when allowing connectivity at altitudes as low as 2,300 masl (Fig. 2). These populations were thus more likely to have been founded by long distance colonisation, as opposed to climate mediated gene flow with other populations.

Results for both species are consistent with population differentiation being influenced by the landscape matrix among mountain peaks, and historical habitat connectivity patterns associated with this. In particular, the connectivity that occurred during the likely glacial distribution of each species. This fits the prediction of gene flow occurring during glacial periods. The importance of the topographic matrix connecting mountains is noteworthy, as even during their glacial extension species seem to have maintained a fragmented (island-like) distribution (Fig. 2). Therefore glacial admixture is expected to have occurred more readily among certain population clusters (e.g. Tláloc-Iztaccihuatl-Popocatepetl, Fig. 2), while other populations should have remained isolated during interglacial stages.

Population differentiation and persistence under a sky-island dynamic

Our analyses of historical habitat distribution, together with genetic differentiation and demographic history of two high altitude plant species, support a sky-island dynamic within the TMVB that has promoted population differentiation and long-term *in-situ* persistence. The niche modelling demonstrates that since their emergence during the last 1.5 Myr (Ferrari *et al.* 2012), the highest volcanoes of the TMVB have provided stable conditions throughout glacial-interglacial cycles suitable for continuous population persistence for subalpine and alpine taxa.

533 The genetic data supports a scenario of long-term population persistence in both
534 species. Genomic differentiation was significant among all populations, with F_{ST} values
535 typically greater than 0.05 (Table S2.1 and S2.2), which is congruent with populations
536 diverging in allele frequencies and accumulating private alleles through the effects of
537 genetic drift and mutation, and absence (or very reduced amounts) of gene flow (Table 1).
538 In addition to differentiation, a demographic syndrome of either limited population
539 expansion or constant size was inferred for most populations of both species (Table 3).
540 Although we could not estimate the absolute timing of demographic events, we can infer
541 that the limited expansions occurred synchronously. This suggests that, in this topographic
542 context, populations from both species have undergone similar responses to environmental
543 change.

544 Inferences of population size constancy, or only limited expansion, points to a
545 demographic history of relative stability and are congruent with a sky-islands scenario for
546 the TVBM for two reasons. First, suitable habitat is expected to have persisted in situ within
547 the TMVB for both focal species during climate fluctuations (Fig. 3), thus allowing for *in situ*
548 population persistence. Second, estimated glacial ranges are not much larger than
549 interglacial ranges (Fig. 2; Fig. 3), which predicts only limited population size change
550 through a glacial cycle. More substantial demographic change is expected for species from
551 lower altitudes of the Mexican highlands (Mastretta-Yanes *et al.* 2015a), and for taxa with
552 more northern distributions (Hewitt 1996; Stewart *et al.* 2010), where species contracted
553 or expanded across large horizontal distances during the Last Glacial Maxima to the
554 present.

555

Conservation and management implications

Most of the sampled mountains of this study are Natural Protected Areas (NPA) currently under different threats and management methods. Our results highlight the conservation value of the TMVB peaks, showing that they are areas of long-term biodiversity persistence despite historical climate fluctuations. Our results are also relevant for the management of these NPA. Firstly, because we show that these mountain peaks behave like islands showing high levels of genetic isolation. As a consequence, we suggest that these mountains should be managed like islands, for instance promoting the use of native germplasm for reforestation efforts. Secondly, our results show that alpine grasslands from the TMVB are a natural ecosystem that has historically persisted within these mountains. Therefore the aforestation of these grasslands, as currently done in some of the mountains, is destroying a natural ecosystem of conservation importance.

Conclusion

We have shown that: (1) the highest stratovolcanoes of the TMVB facilitated the existence of timberline-alpine grasslands throughout glacial/interglacial cycles (long-term *in situ* population persistence); and (2) population genetic differentiation of species from this ecosystem can be explained by the degree of habitat connectivity among mountains during the glacial periods.

Similar scenarios have been postulated for taxa of the TMVB from lower altitudes using classical population genetic and phylogeographic approaches (e.g. McCormack *et al.* 2008; Bryson *et al.* 2011, 2012; Gutiérrez-Rodríguez *et al.* 2011; Ornelas *et al.* 2013; Parra-Olea *et al.* 2012). Some of these previous phylogeographic studies focusing on divergence

579 times (e.g. Ornelas *et al.* 2010; Bryson *et al.* 2012a; b; Leaché *et al.* 2013) have not been
580 able to distinguish between the confounding effects of climate and geological change,
581 because in the TMVB climate fluctuations and volcanic changes co-occurred during the
582 Pleistocene (Mastretta-Yanes et al. 2015). However, here we assessed present versus past
583 historical connectivity quantitatively and in a landscape explicit context. This spatial
584 approach allows to relate population differentiation to the Pleistocene glacial cycles and
585 the sky-island dynamics they produce in tropical mountains.

586 Our results support the ongoing role of tropical mountains as cradles for
587 biodiversity by uncovering cryptic differentiation and limits to gene flow, and as museums
588 for biodiversity by promoting long-term *in situ* persistence. Therefore, the conservation
589 importance of tropical mountains, such as the ones of the TMVB, resides not only on its
590 species richness *per se*, but on that landscapes like these promote both long-term
591 population survival and further diversification.

592

593 **Acknowledgments**

594 Part of the analyses were carried out on the High Performance Computing Cluster
595 supported by the Research and Specialist Computing Support service at UEA. Field work
596 was possible thanks to Oscar Trejo from DGFS and CONANP staff from the natural
597 protected areas Cofre de Perote, Pico de Orizaba, La Malinche, Izta-Popo, Nevado de Toluca,
598 Mariposa Monarca, Pico de Tancítaro and Nevado de Colima. We are thankful to SMG,
599 JRPPK, JJRL, AOM, ROF, SSF, RAF, TSA, JAA, FDRG, FQB and MJLF for fieldwork assistance
600 and to T. Wyss, A. Brelsford and C. Berney for laboratory work assistance. We acknowledge
601 the international modelling groups for providing their data for analysis, the Laboratoire

des Sciences du Climat et de l'Environnement (LSCE) for collecting and archiving the model data. The PMIP 2 Data Archive is supported by CEA, CNRS and the Programme National d'Etude de la Dynamique du Climat (PNEDC). The analyses were performed using version 01/20/10 of the database. More information is available on http://pmip2.lsce.ipsl.fr/. This work was supported by Consejo Nacional de Ciencia y Tecnología (grant number CONACYT 213538 to AMY and CONACYT 178245 to DP), and by Rosemary Grant Award for Graduate Student Research from the Society for the Study of Evolution granted to AMY.

References

Adams RP (2014) *Junipers of the world: The genus Juniperus*. Trafford Publishing.

Almeida-Leñero, L., Escamilla, M., Giménez de Azcárate, J., González-Trápaga, A., Cleff, A. M. (2007) Vegetación alpina de los volcanes Popocatépetl, Iztaccíhuatl y Nevado de Toluca. In: *Biodiversidad de la faja volcánica Trans-Mexicana* (eds Luna-Vega I, Morrone JJ, Espinosa D), pp. 179–198. Universidad Nacional Autónoma de México, Facultad de Estudios Superiores Zaragoza e Instituto de Biología.

Araújo MB, Guisan A (2006) Five (or so) challenges for species distribution modelling. *Journal of Biogeography*, **33**, 1677–1688.

Beaman JH (1962) The Timberlines of Iztaccihuatl and Popocatepetl, Mexico. *Ecology*, **43**, 377–385.

Bonner FT (2008) Juniperus L. juniper. In: *Seeds of woody plants in the United States* Agriculture Handbook. (eds Bonner FT, Karrfalt RP), pp. 607–614. USDA Forest Service.

Braconnot P, Otto-Bliesner B, Harrison S *et al.* (2007) Results of PMIP2 coupled simulations of the Mid-Holocene and Last Glacial Maximum – Part 1: experiments and large-scale features. *Clim. Past*, **3**, 261–277.

Bryson RW, García-Vázquez UO, Riddle BR (2012a) Relative roles of Neogene vicariance and Quaternary climate change on the historical diversification of bunchgrass lizards (Sceloporus scalaris group) in Mexico. *Molecular Phylogenetics and Evolution*, **62**, 447–457.

Bryson RW, García-Vázquez UO, Riddle BR (2012b) Diversification in the Mexican horned lizard Phrynosoma orbiculare across a dynamic landscape. *Molecular Phylogenetics and Evolution*, **62**, 87–96.

Bryson RW, Murphy RW, Lathrop A, Lazcano-Villareal D (2011) Evolutionary drivers of phylogeographical diversity in the highlands of Mexico: a case study of the Crotalus triseriatus species group of montane rattlesnakes. *Journal of Biogeography*, **38**, 697–710.

Caballero-Rodríguez D, Lozano-García S, Correa-Metrio A (2017) Vegetation assemblages of central Mexico through the late Quaternary: modern analogs and compositional turnover. *Journal of Vegetation Science*, doi:10.1111/jvs.12515.

Cadena CD, Kozak KH, Gómez JP *et al.* (2011) Latitude, elevational climatic zonation and speciation in New World vertebrates. *Proceedings of the Royal Society B: Biological Sciences*, rspb20110720.

Calderón de Rzedowski G, Rzedowski J (2005) *Flora Fanerogámica del Valle de México*. Instituto de Ecología A.C. y Comisión Nacional para el Conocimiento y Uso de la Biodiversidad, Pátzcuaro, Michoacán, México.

Carnaval AC, Hickerson MJ, Haddad CFB, Rodrigues MT, Moritz C (2009) Stability predicts genetic diversity in the Brazilian Atlantic forest hotspot. *Science*, **323**, 785 –789.

Catchen J, Amores A, Hohenlohe P, Cresko W, Postlethwait JH (2011) Stacks: building and genotyping loci *de novo* from short-read sequences. *G3: Genes, Genomes, Genetics*, **1**, 171–182.

Catchen J, Hohenlohe PA, Bassham S, Amores A, Cresko WA (2013) Stacks: an analysis tool set for population genomics. *Molecular Ecology*, **22**, 3124–3140.

Csilléry K, François O, Blum MGB (2012) abc: an R package for approximate Bayesian computation (ABC). *Methods in Ecology and Evolution*, **3**, 475–479.

Devitt TJ, Devitt SEC, Hollingsworth BD, McGuire JA, Moritz C (2013) Montane refugia predict population genetic structure in the Large-blotched Ensatina salamander. *Molecular Ecology*, **22**, 1650–1665.

Dray S, Dufour A-B (2007) The ade4 package: implementing the duality diagram for ecologists. *Journal of statistical software*, **22**, 1–20.

Excoffier L, Dupanloup I, Huerta-Sánchez E, Sousa VC, Foll M (2013) Robust Demographic Inference from Genomic and SNP Data. *PLOS Genet*, **9**, e1003905.

Felsenstein J (1971) Inbreeding and Variance Effective Numbers in Populations with Overlapping Generations. *Genetics*, **68**, 581–597.

Ferrari L, Orozco-Esquivel T, Manea V, Manea M (2012) The dynamic history of the Trans-Mexican Volcanic Belt and the Mexico subduction zone. *Tectonophysics*, **522–523**, 122–149.

Fjeldså J, Bowie RCK (2008) New perspectives on the origin and diversification of Africa's forest avifauna. *African Journal of Ecology*, **46**, 235–247.

Fjeldså J, Bowie RCK, Rahbek C (2012) The Role of Mountain Ranges in the Diversification of Birds. *Annual Review of Ecology, Evolution, and Systematics*, **43**, 249–265.

Fjeldså J, Lambin E, Mertens B (1999) Correlation between endemism and local ecoclimatic stability documented by comparing Andean bird distributions and remotely sensed land surface data. *Ecography*, **22**, 63–78.

Francis JK (2004) Mahonia aquifolium (Pursh) Nutt. *Wildland shrubs of the United States and its territories: thamnic descriptions*, **1**, 461.

Graham CH, Moritz C, Williams SE (2006) Habitat history improves prediction of biodiversity in rainforest fauna. *Proceedings of the National Academy of Sciences of the United States of America*, **103**, 632–636.

Gutiérrez-Rodríguez C, Ornelas JF, Rodríguez-Gómez F (2011) Chloroplast DNA phylogeography of a distylous shrub (Palicourea padifolia, Rubiaceae) reveals past fragmentation and demographic expansion in Mexican cloud forests. *Molecular Phylogenetics and Evolution*, **61**, 603–615.

683 Gutenkunst RN, Hernandez RD, Williamson SH, Bustamante CD (2009) Inferring the Joint
684 Demographic History of Multiple Populations from Multidimensional SNP Frequency
685 Data. *PLOS Genet*, **5**, e1000695.
686 Hewitt GM (1996) Some genetic consequences of ice ages, and their role in divergence and
687 speciation. *Biological Journal of the Linnean Society*, **58**, 247–276.
688 Hijmans RJ, Cameron SE, Parra JL, Jones PG, Jarvis A (2005) Very high resolution
689 interpolated climate surfaces for global land areas. *International Journal of Climatology*,
690 **25**.
691 Hugall A, Moritz C, Moussalli A, Stanisic J (2002) Reconciling paleodistribution models and
692 comparative phylogeography in the Wet Tropics rainforest land snail Gnarosophia
693 bellendenkerensis (Brazier 1875). *Proceedings of the National Academy of Sciences of*
694 *the United States of America*, **99**, 6112 –6117.
695 Jetz W, Rahbek C (2002) Geographic range size and determinants of avian species richness.
696 *Science*, **297**, 1548 –1551.
697 Jetz W, Rahbek C, Colwell RK (2004) The coincidence of rarity and richness and the
698 potential signature of history in centres of endemism. *Ecology Letters*, **7**, 1180–1191.
699 Kessler M (2002) The elevational gradient of Andean plant endemism: varying influences
700 of taxon-specific traits and topography at different taxonomic levels. *Journal of*
701 *Biogeography*, **29**, 1159–1165.
702 Krömer T, Acebey A, Kluge J, Kessler M (2013) Effects of altitude and climate in
703 determining elevational plant species richness patterns: A case study from Los Tuxtlas,
704 Mexico. *Flora - Morphology, Distribution, Functional Ecology of Plants*, **208**, 197–210.
705 Kruckeberg AR, Rabinowitz D (1985) Biological aspects of endemism in higher plants.
706 *Annual Review of Ecology and Systematics*, **16**, 447–479.
707 Lauer W (1978) Timberline studies in Central Mexico. *Arctic and Alpine Research*, **10**, 383.
708 Leaché AD, Palacios JA, Minin VN, Bryson RW (2013) Phylogeography of the Trans-Volcanic
709 bunchgrass lizard (*Sceloporus bicanthalis*) across the highlands of south-eastern
710 Mexico. *Biological Journal of the Linnean Society*, **110**, 852–865.
711 Lee-Yaw JA, Davidson A, McRae BH, Green DM (2009) Do landscape processes predict
712 phylogeographic patterns in the wood frog? *Molecular Ecology*, **18**, 1863–1874.
713 Liaw A, Wiener M (2002) Classification and Regression by randomForest. *R News*, **2**, 18–22.
714 Loarie SR, Duffy PB, Hamilton H *et al.* (2009) The velocity of climate change. *Nature*, **462**,
715 1052–1055.
716 Lozano-García MS, Ortega-Guerrero B (1994) Palynological and magnetic susceptibility
717 records of Lake Chalco, central Mexico. *Palaeogeography, Palaeoclimatology,*
718 *Palaeoecology*, **109**, 177–191.
719 Lozano-García MS, Ortega-Guerrero B (1998) Late Quaternary environmental changes of
720 the central part of the Basin of Mexico; correlation between Texcoco and Chalco basins.
721 *Review of Palaeobotany and Palynology*, **99**, 77–93.
722 Lozano-García S, Sosa-Nájera S, Sugiura Y, Caballero M (2005) 23,000 yr of vegetation
723 history of the Upper Lerma, a tropical high-altitude basin in Central Mexico. *Quaternary*
724 *Research*, **64**, 70–82.
725 Lozano-García S, Vázquez-Selem L (2005) A high-elevation Holocene pollen record from
726 Iztaccihuatl volcano, central Mexico. *The Holocene*, **15**, 329–338.

Mastretta-Yanes A, Moreno-Letelier A, Piñero D, Jorgensen TH, Emerson BC (2015a) Biodiversity in the Mexican highlands and the interaction of geology, geography and climate within the Trans-Mexican Volcanic Belt. *Journal of Biogeography*, 1586–1600.

Mastretta-Yanes A, Arrigo N, Alvarez N *et al.* (2015b) Data from: RAD sequencing, genotyping error estimation and de novo assembly optimization for population genetic inference. *Dryad Digital Repository.*, doi:10.5061/dryad.g52m3.

Mastretta-Yanes A, Arrigo N, Alvarez N *et al.* (2015c) Restriction site-associated DNA sequencing, genotyping error estimation and de novo assembly optimization for population genetic inference. *Molecular Ecology Resources*, **15**, 28–41.

Mastretta-Yanes A, Zamudio S, Jorgensen TH *et al.* (2014) Gene duplication, population genomics and species-level differentiation within a tropical mountain shrub. *Genome Biology and Evolution*, evu205.

McCormack JE, Peterson AT, Bonaccorso E, Smith TB (2008) Speciation in the highlands of Mexico: genetic and phenotypic divergence in the Mexican jay (*Aphelocoma ultramarina*). *Molecular Ecology*, **17**, 2505–2521.

McRae BH (2006) Isolation by resistance. *Evolution*, **60**, 1551-1561.

McRae BH, Beier P (2007) Circuit theory predicts gene flow in plant and animal populations. *Proceedings of the National Academy of Sciences*, **104**, 19885 –19890.

McRae BH, Dickson BG, Keitt TH, Shah VB (2008) Using circuit theory to model connectivity in ecology, evolution, and conservation. *Ecology*, **89**, 2712–2724.

Moore JA, Tallmon DA, Nielsen J, Pyare S (2011) Effects of the landscape on boreal toad gene flow: does the pattern–process relationship hold true across distinct landscapes at the northern range margin? *Molecular Ecology*, **20**, 4858–4869.

Myers N, Mittermeier RA, Mittermeier CG, da Fonseca GAB, Kent J (2000) Biodiversity hotspots for conservation priorities. *Nature*, **403**, 853–858.

Ohlemüller R, Anderson BJ, Araújo MB *et al.* (2008) The coincidence of climatic and species rarity: high risk to small-range species from climate change. *Biology Letters*, **4**, 568–572.

Oksanen J, Blanchet FG, Friendly M et al. (2016) vegan: Community Ecology Package. http://CRAN.R-project.org/package=vegan

Ornelas JF, Ruiz-Sánchez E, Sosa V (2010) Phylogeography of *Podocarpus matudae* (Podocarpaceae): pre-Quaternary relicts in northern Mesoamerican cloud forests. *Journal of Biogeography*, **37**, 2384–2396.

Ornelas JF, Sosa V, Soltis DE *et al.* (2013) Comparative phylogeographic analyses illustrate the complex evolutionary history of threatened cloud forests of Northern Mesoamerica. *PLoS ONE*, **8**, e56283.

Orsini L, Vanoverbeke J, Swillen I, Mergeay J, De Meester L (2013) Drivers of population genetic differentiation in the wild: isolation by dispersal limitation, isolation by adaptation and isolation by colonization. *Molecular Ecology*, **22**, 5983-5999.

Päckert M, Martens J, Sun Y-H *et al.* (2012) Horizontal and elevational phylogeographic patterns of Himalayan and Southeast Asian forest passerines (Aves: Passeriformes). *Journal of Biogeography*, **39**, 556–573.

Paradis E, Claude J, Strimmer K (2004) APE: Analyses of Phylogenetics and Evolution in R language. *Bioinformatics*, **20**, 289–290.

Parchman TL, Gompert Z, Mudge J *et al.* (2012) Genome-wide association genetics of an adaptive trait in lodgepole pine. *Molecular Ecology*, **21**, 2991–3005.

Parra-Olea G, Windfield JC, Velo-Antón G, Zamudio KR (2012) Isolation in habitat refugia promotes rapid diversification in a montane tropical salamander. *Journal of Biogeography*, **39**, 353–370.
Peterson BK, Weber JN, Kay EH, Fisher HS, Hoekstra HE (2012) double digest radseq: an inexpensive method for de novo SNP discovery and genotyping in model and non-model species. *PLoS ONE*, **7**, e37135.
Peterson PDJ (2003) The Common Barberry: The Past and Present Situation in Minnesota and the Risk of Wheat Stem Rust Epidemics. PhD Thesis. North Carolina State University.
Prates I, Xue AT, Brown JL *et al.* (2016) Inferring responses to climate dynamics from historical demography in neotropical forest lizards. *Proceedings of the National Academy of Sciences*, **113**, 7978–7985.
Phillips SJ, Anderson RP, Schapire RE (2006) Maximum entropy modeling of species geographic distributions. *Ecological Modelling*, **190**, 231–259.
Rahbek C, Gotelli NJ, Colwell RK *et al.* (2007) Predicting continental-scale patterns of bird species richness with spatially explicit models. *Proceedings of the Royal Society B: Biological Sciences*, **274**, 165–174.
R. Core Team (2012) *R: A Language and Environment for Statistical Computing*. R Foundation for Statistical Computing, Vienna, Austria.
Roberts DR, Hamann A (2012) Method selection for species distribution modelling: are temporally or spatially independent evaluations necessary? *Ecography*, **35**, 792–802.
Rounsaville TJ, Ranney TG (2010) Ploidy levels and genome sizes of *Berberis* L. and *Mahonia* nutt. species, hybrids, and cultivars. *HortScience*, **45**, 1029–1033.
Rousset F (1997) Genetic differentiation and estimation of gene flow from F-statistics under isolation by distance. *Genetics*, **145**, 1219–1228.
Rzedowski J (1978) *Vegetación de México*. Limusa, México.
Sandel B, Arge L, Dalsgaard B *et al.* (2011) The influence of late Quaternary climate-change velocity on species endemism. *Science*, **334**, 660 –664.
Smith BT, McCormack JE, Cuervo AM *et al.* (2014) The drivers of tropical speciation. *Nature*, doi: 10.1038/nature13687
Stewart JR, Lister AM, Barnes I, Dalén L (2010) Refugia revisited: individualistic responses of species in space and time. *Proceedings of the Royal Society B: Biological Sciences*, **277**, 661–671.
Toledo V (1982) Pleistocene changes of vegetation in tropical Mexico. In: *Biological diversification in the tropics* (ed Prance GT), pp. 93–111. Columbia University Press, New York.
Vázquez-Selem L, Heine K (2011) Late Quaternary Glaciation in Mexico. In: *Quaternary Glaciations - Extent and Chronology - A Closer Look* (eds Ehlers J, Gibbard PL, Hughes P), pp. 849–861. Elsevier.
Wang IJ (2013) Examining the full effects of landscape heterogeneity on spatial genetic variation: a multiple matrix regression approach for quantifying geographic and ecological isolation. *Evolution*, **67**, 3403–3411.
Webb T, Bartlein PJ (1992) Global changes during the last 3 million years: climatic controls and biotic responses. *Annual Review of Ecology and Systematics*, **23**, 141–173.
Weir JT (2009) Implications of genetic differentiation in Neotropical montane forest birds. *Annals of the Missouri Botanical Garden*, **96**, 410–433.

Wickham H, Chang W (2013) *ggplot2: An implementation of the Grammar of Graphics*. v. 0.9.3.1. CRAN repository.
Xue AT, Hickerson MJ (2015) The aggregate site frequency spectrum (aSFS) for comparative population genomic inference. *Molecular Ecology*, **24**, 6223–6240.
Xue AT, Hickerson MJ (under review) Multi-DICE: R package for comparative population genomic inference under multi-taxa hierarchical co-demographic models.
Zonneveld BJM (2012) Conifer genome sizes of 172 species, covering 64 of 67 genera, range from 8 to 72 picogram. *Nordic Journal of Botany*.

Data Accessibility

This project has been deposited at Dryad Repository under the accession XXXXXXX. The repository includes lab protocol, species occurrence data, spatial data, genetic data in plink format and the scripts used for all analyses. Raw RADseq data is at the Sequence Read Archive (SRA) accession SRP035472 for *Berberis* and XXXXXX for *Juniperus.*

Author Contributions

AMY, DP, THJ and BCE conceived and designed the study. AMY performed fieldwork and laboratory work, assembled the RAD data and made all analyses, except for the aSFS and the ecosystem distribution modelling. ATX performed the aSFS analyses. AML performed the ecosystem distribution modelling. NA and THJ supervised lab work and preliminary analyses. AMY, DP and BCE lead manuscript writing. All authors contributed to the discussion and manuscript writing.

Table 1. Summary population genetic statistics for *B. alpina* and *J. monticola*

Pop. ID	*Ns*	*N*	Priv.	Sites	P	H_{obs}	π	F_{IS}
B. alpina								
Pe	6	6.11	1101	2183	0.9108	0.1234	0.1395	0.0374
Tl	10	4.76	332	1557	0.9383	0.0917	0.1020	0.0235
Ma	10	6.42	503	1743	0.9338	0.0967	0.1060	0.0219
Iz	8	8.03	375	1708	0.9404	0.0924	0.0951	0.0141
Aj	8	8.54	477	1892	0.9357	0.1006	0.1025	0.0073
To	8	6.31	326	1376	0.9449	0.0908	0.0883	0.0004
J. monticola								
Ch	8	7.03	608	2691	0.9421	0.0689	0.0936	0.0650
Pe	5	4.04	206	1569	0.9549	0.0577	0.0741	0.0326
Ci	10	9.06	176	2189	0.9515	0.0583	0.0757	0.0465
Ne	10	8.70	177	2236	0.9522	0.0582	0.0756	0.0460
Ma	9	7.27	175	1842	0.9543	0.0487	0.0713	0.0564
Tl	10	8.81	324	2646	0.9461	0.0661	0.0860	0.0554
Iz	8	6.64	265	2337	0.9482	0.0651	0.0844	0.0492
Pp	8	7.00	208	2190	0.9497	0.0587	0.0804	0.0553
Aj	7	4.90	194	1812	0.9515	0.0505	0.0785	0.0622
To	8	6.13	154	1673	0.9549	0.0495	0.0706	0.0491
Bl	9	7.62	327	2260	0.9486	0.0626	0.0808	0.0468
Ta	10	8.40	431	2298	0.9467	0.0594	0.0826	0.0580
Co	8	5.37	309	1994	0.9477	0.0508	0.0849	0.0777

Results include only nucleotide positions that are polymorphic in at least one population. The first column shows the number of individuals per population that were used for the analysis (Ns). Next are the average number of individuals genotyped at each locus (N), the number of variable sites unique to each population (i.e. private alleles, Priv.), the number of polymorphic nucleotide sites for that population (Sites), the average frequency of the major allele (P), the average observed heterozygosity per locus (H_{obs}), the average nucleotide diversity (π), and the average Wright's inbreeding coefficient (F_{IS}). Populations are ordered East to West, top to bottom. Population IDs as in Fig. 1.

Table 2. Isolation by resistance

	B. alpina		*J. monticola* all pops.		*J. monticola* excluding Co & Ta	
Surface	***r***	**Pt *r***	***r***	**Pt *r***	***r***	**Pt *r***
present	0.787**	0.059 NS	0.469 *	-0.034 NS	0.662 ***	0.406**
ccsm	0.662*	-0.061 NS	0.402 *	-0.140 NS	<u>0.686</u> ***	<u>0.453</u>**
miroc	0.792**	0.218 NS	0.430 *	-0.129 NS	0.675 ***	0.427**
flat	0.881**	- -	<u>0.499</u> *	- -	0.579 ***	--
1,800	0.888**	0.244 NS	0.327 NS	-0.374 NS	0.575 ***	0.087NS
2,000	0.893***	0.307 NS	0.299 NS	-0.376 NS	0.566 ***	0.052NS
2,300	0.827**	0.311 NS	0.319 NS	-0.343 NS	0.555 ***	0.022NS
2,500	0.901**	0.417 NS	0.384 NS	-0.285 NS	0.530 **	0.005NS
2,700	0.929**	0.620 *	0.443 *	-0.159 NS	0.550 ***	0.068NS
3,000	<u>0.940</u>**	<u>0.717</u> *	0.374 *	-0.184 NS	0.331 NS	-0.188NS
3,300	0.905**	0.435 NS	0.389 *	-0.180 NS	0.353 NS	-0.230NS
3,500	0.833**	0.023 NS	0.386 *	-0.149 NS	0.34 NS	-0.272NS
4,000	0.681*	-0.017 NS	0.378 *	-0.201 NS	0.335 NS	-0.249NS

Associations between genetic differentiation (linearized F_{ST}, see main text) and pairwise effective distances at different surfaces (see Fig. 2 for an explanation of these). Mantel test *r* value (*r*) and Partial Mantel test *r* value (Pt *r*) are reported for each species. Significance codes are as follows: < 0.001 '***', <0.01 '**', < 0.05 '*', and not significant 'NS'. Underlined cells correspond to the surface with the highest prediction value for each taxon.

Table 3. Proportion of populations in synchrony and number of synchronous pulses.

Estimation method	ζ			ψ		
	res	***r***	***rmse***	**res**	***r***	***rmse***
hRF Hyperparameter Estimation	0.821	0.613	0.229	1.81	0.784	0.70
hABC Hyperparameter Estimation - Median	0.929	0.610	0.236	1.00	0.761	0.92
hABC Hyperparameter Estimation - Mode	0.999	0.561	0.303	1.00	0.619	1.05

Results for the downprojection to four individuals, see Table S2.4 for results with the downprojection to five. **ζ**: proportion of populations in synchrony (considering both species together). **ψ**: number of synchronous pulses. For **ζ** and **ψ,** the three columns show the resulting estimation (res), and the cross-validation accuracy check based on the correlation (*r*) and the root mean squared error (*rmse*) between the simulated true values and the estimated values.

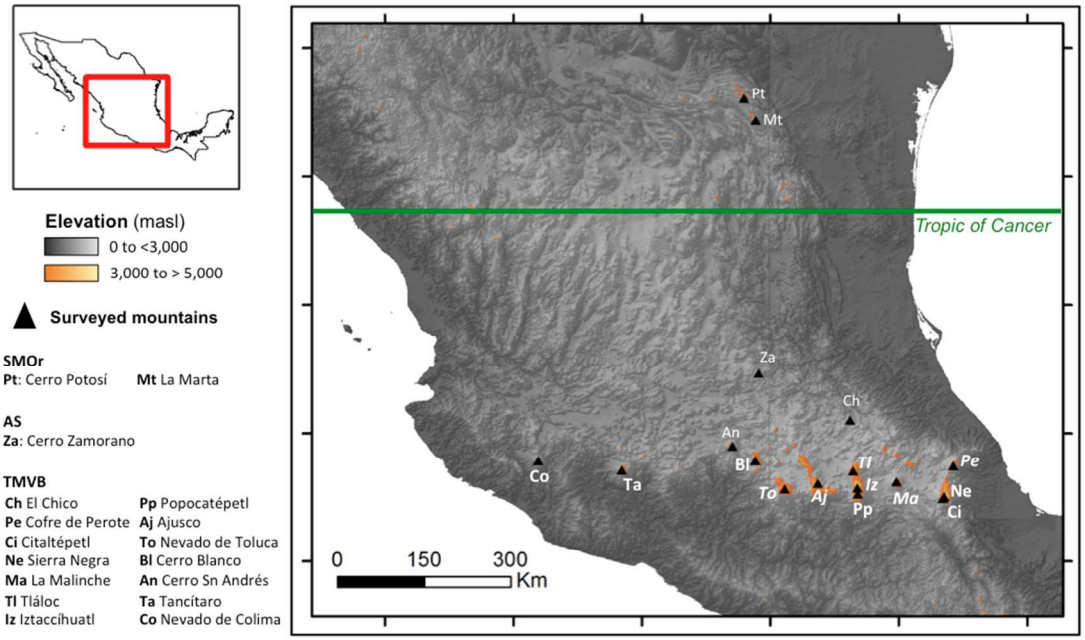

Figure 1. High elevation mountains with timberline - alpine grasslands surveyed (triangles) for *Berberis alpina* and *Juniperus monticola* in the Sierra Madre Oriental (SMOr), the Altiplano Sur (AS) and the Transmexican Volcanic Belt (TMVB). *Berberis alpina* was found in populations Pe, Ma, Tl, Iz, Aj and To (italics) and *Juniperus monticola* was in populations Ch, Pe, Ci, Ne, Ma, Tl, Iz, Pp, Aj, To, Bl, Ta and Co (bold).

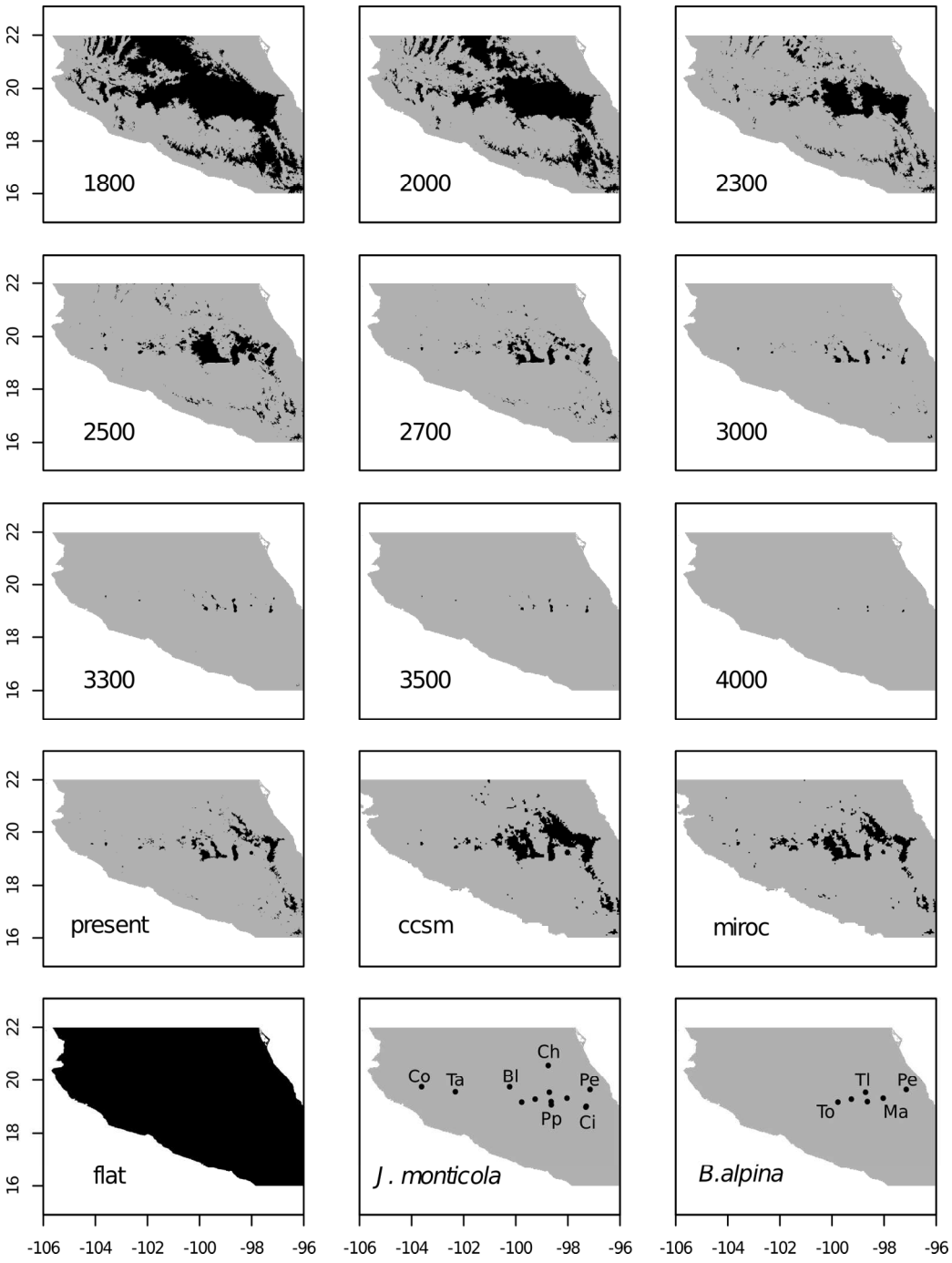

Figure 2. Resistance surfaces used to estimate effective distances among populations. Areas allowing the highest gene flow are shown in black. The first three rows show the surfaces using the elevation data; the fourth row uses the distribution modeling for the timberline-alpine grassland for the present and the LGM (CCSM and MIROC layers); the last row shows a landscape where all cells have high conductance ('flat' landscape) and sampling points for *J. monticola* and *B. alpina.* Some mountain names are indicated for reference (ID codes as in Fig. 1). For all panels, numbers on the x and y axes represent latitude and longitude, respectively.

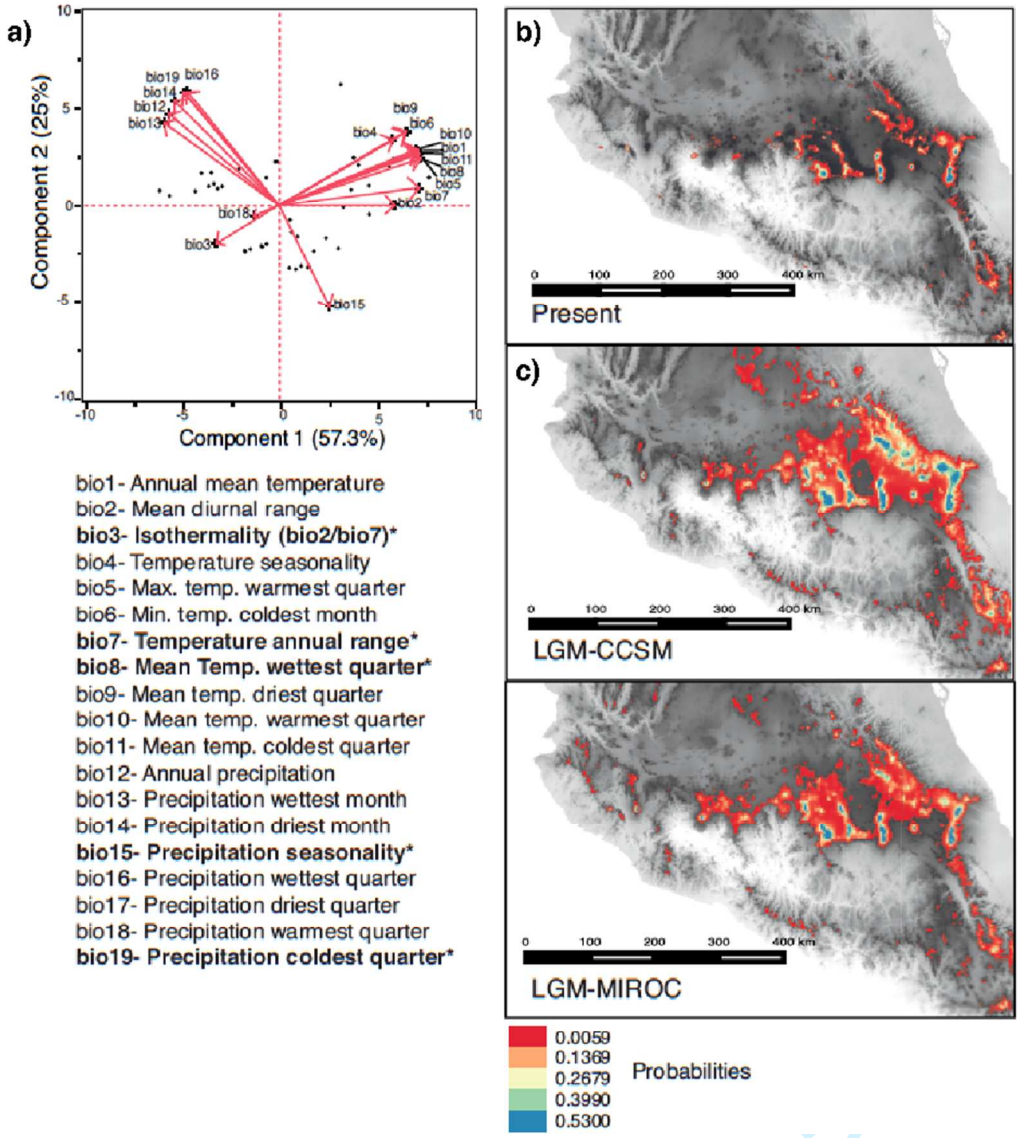

Figure 3. Environmental analyses and distribution models of the timberline - alpine grassland for interglacial and glacial conditions of the TMVB (a) Principal component analysis of 19 bioclimatic variables. The independent variables with the highest contributions to variance were selected for the potential distribution models and are indicated with an asterisk. Potential distribution models of the alpine grassland for the present (b) and Last Glacial Maximum (c). Two sets of environmental layers were used for the projection to the LGM: CCSM and MIROC (details in the methods). The yellow to blue color gradient of *b* indicates areas where the alpine grasslands are known to occur in the present interglacial. Projections to the LGM show that this ecosystem likely occurred in the same mountains, but with a larger distribution extending to lower altitudes.

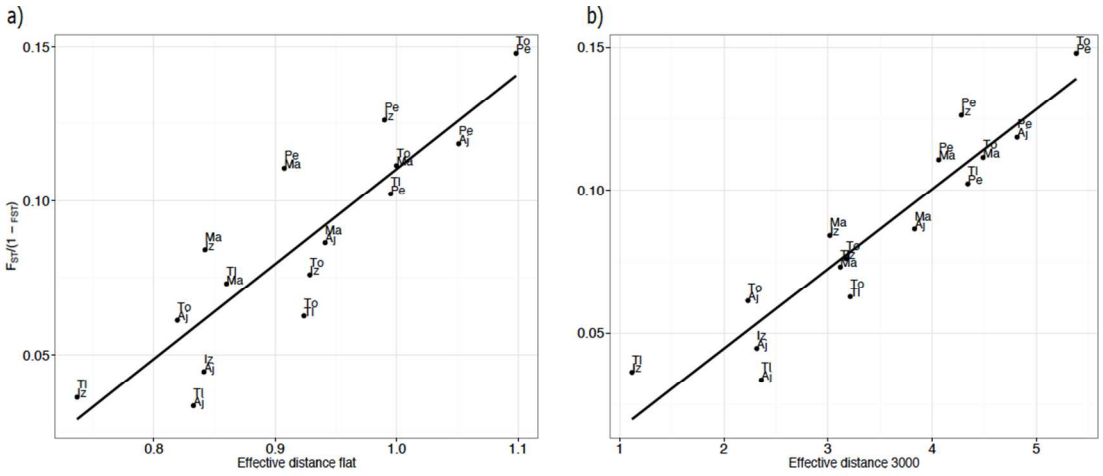

Figure 4. For *B. alpina,* relationship between linearized pairwise F_{ST} and (a) the 'flat' surface (isolation by distance, Mantel r=0.879, p<0.01) and (b) the resistance surface of 3,000 masl, which provided the highest explanatory power (isolation by resistance, Mantel r=0.940, p<0.01, Partial Mantel r=0.717, p<0.05). Labels show populations of each pair-wise comparison. Codes as in Fig. 1.

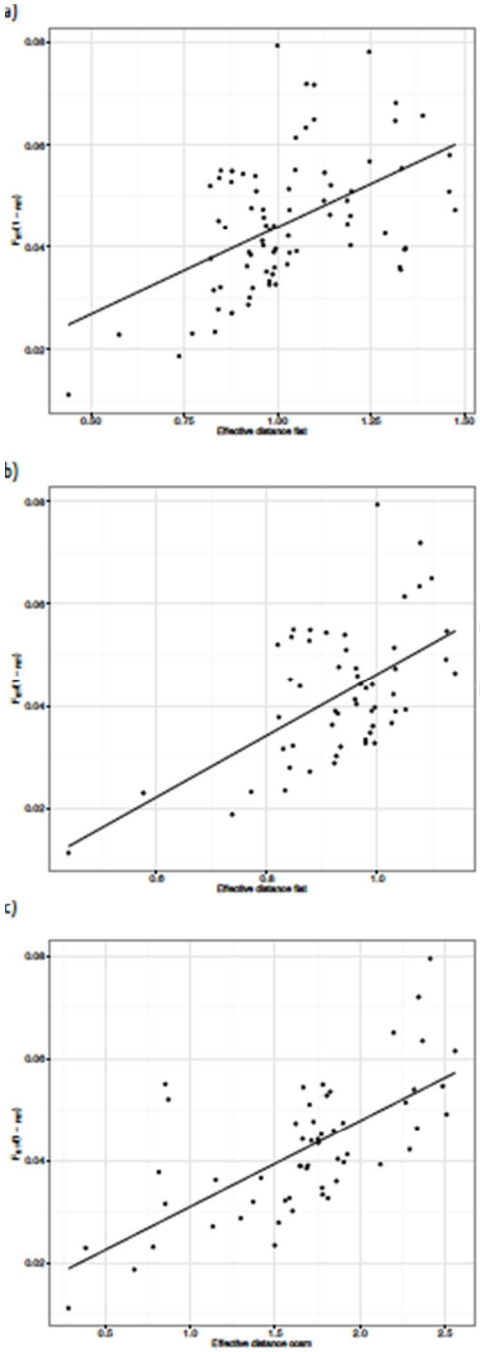

Figure 5. For *J. monticola,* relationship between linearized pairwise F_{ST} and (a) the 'flat' surface including all populations (isolation by distance, Mantel r=0.499, p<0.01) or (b) excluding the Tancítaro and Nevado de Colima populations (isolation by distance, Mantel r=0.579, p<0.001). (c) Relationship between linearized pairwise F_{ST} and the resistance surface of SDM with LGM-CCSM conditions, which provided the highest explanatory power (isolation by resistance, Mantel r=0.686, p<0.001, Partial Mantel r=0.453, p<0.01).

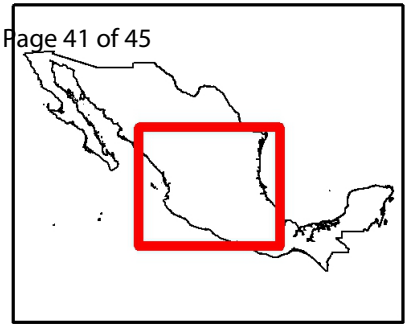

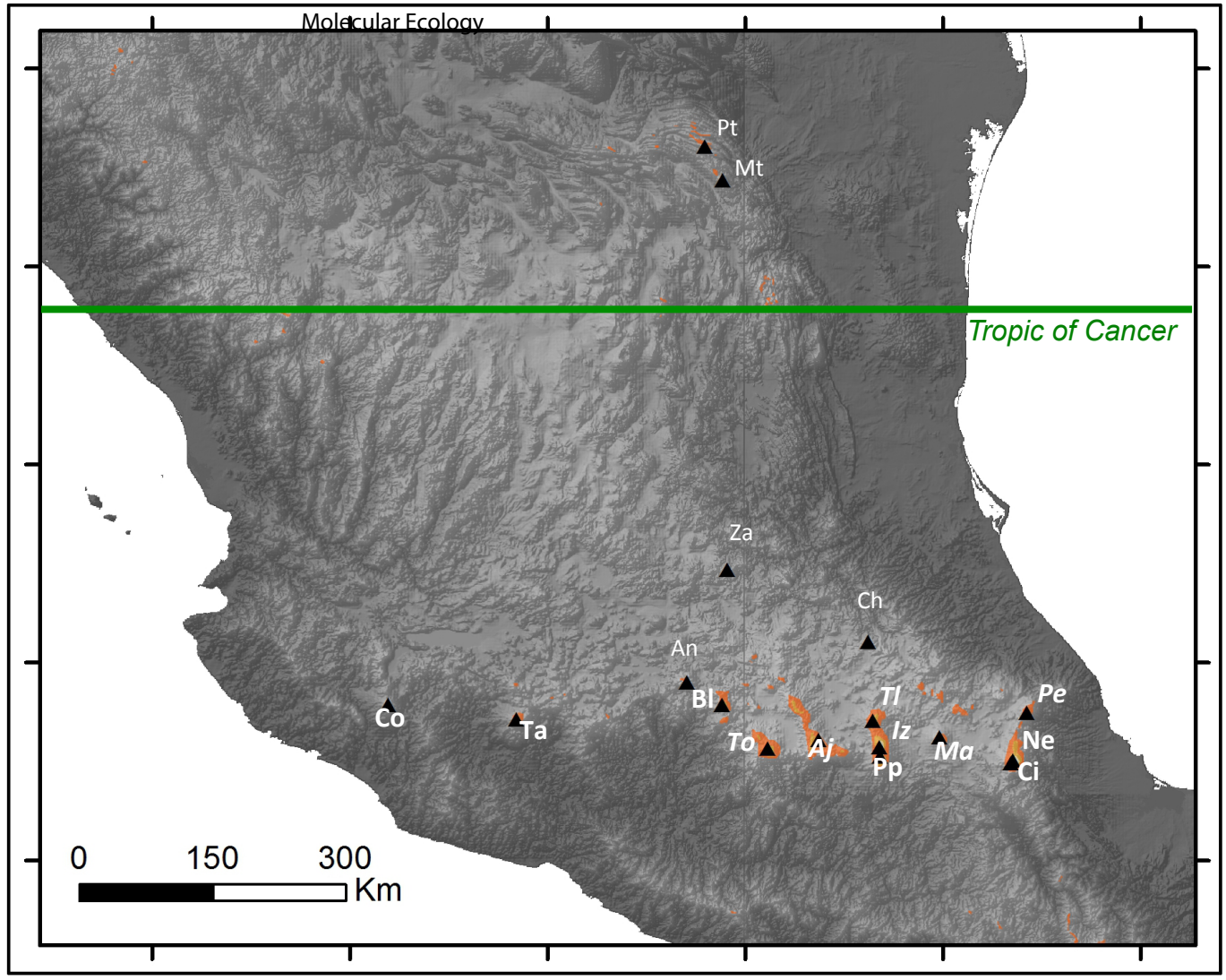

Elevation (masl)

0 to <3,000

3,000 to > 5,000

Surveyed mountains

SMOr

Pt: Cerro Potosí **Mt** La Marta

AS

Za: Cerro Zamorano

TMVB

Ch El Chico
Pe Cofre de Perote
Ci Citaltépetl
Ne Sierra Negra
Ma La Malinche
Tl Tláloc
Iz Iztaccíhuatl
Pp Popocatépetl
Aj Ajusco
To Nevado de Toluca
Bl Cerro Blanco
An Cerro Sn Andrés
Ta Tancítaro
Co Nevado de Colima

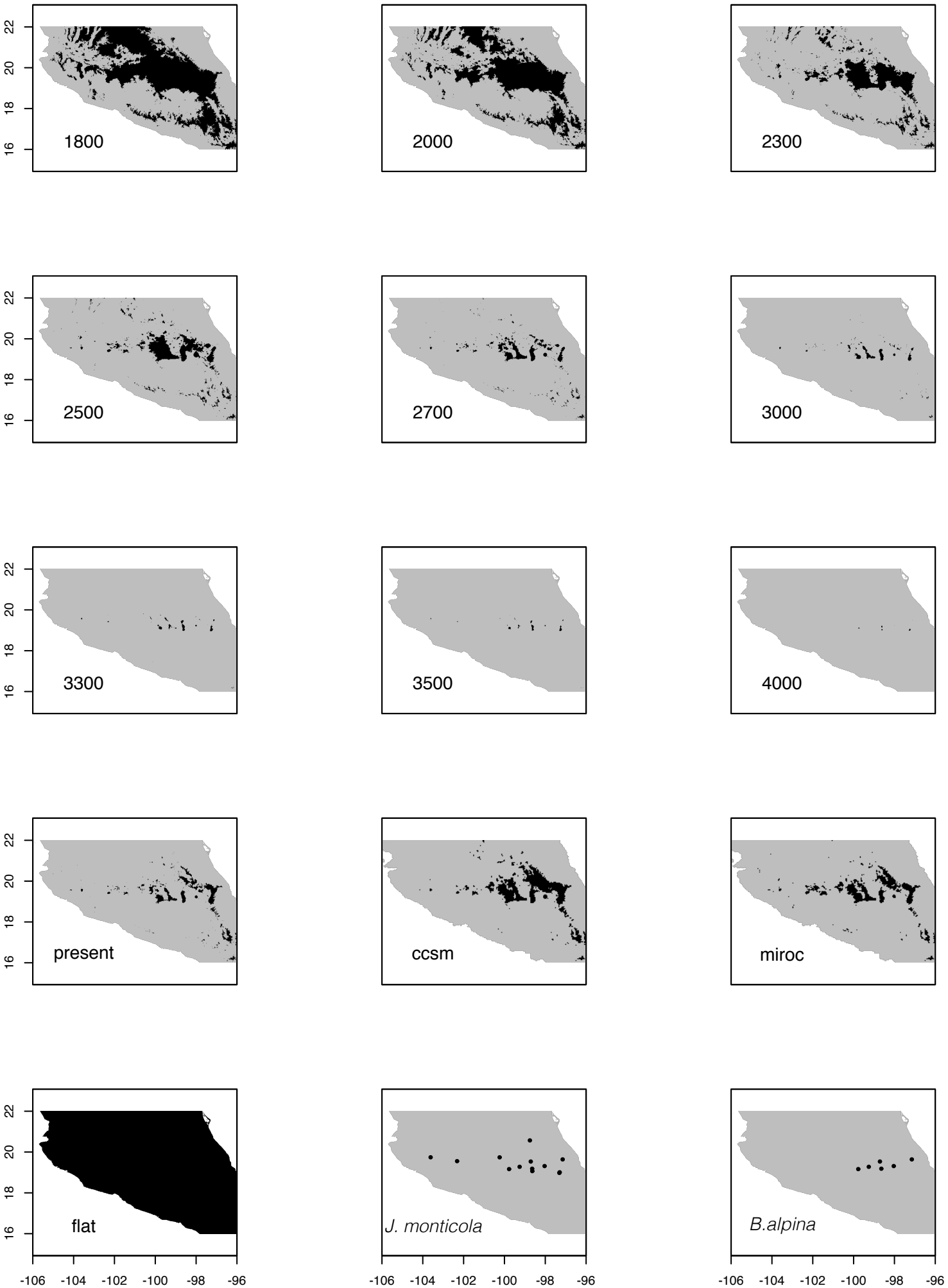
1800
2000
2300
2500
2700
3000
3300
3500
4000
present
ccsm
miroc
flat
J. monticola
B.alpina
22
20
18
16
-106
-104
-102
-100
-98
-96

A)

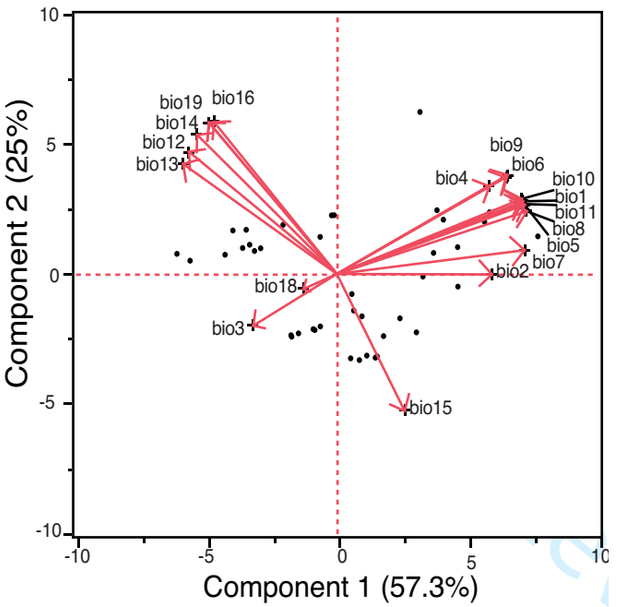

bio1- Annual mean temperature
bio2- Mean diurnal range
bio3- Isothermality (bio2/bio7)*
bio4- Temperature seasonality
bio5- Max. temp. warmest quarter
bio6- Min. temp. coldest month
bio7- Temperature annual range*
bio8- Mean Temp. wettest quarter*
bio9- Mean temp. driest quarter
bio10- Mean temp. warmest quarter
bio11- Mean temp. coldest quarter
bio12- Annual precipitation
bio13- Precipitation wettest month
bio14- Precipitation driest month
bio15- Precipitation seasonality*
bio16- Precipitation wettest quarter
bio17- Precipitation driest quarter
bio18- Precipitation warmest quarter
bio19- Precipitation coldest quarter*

B)

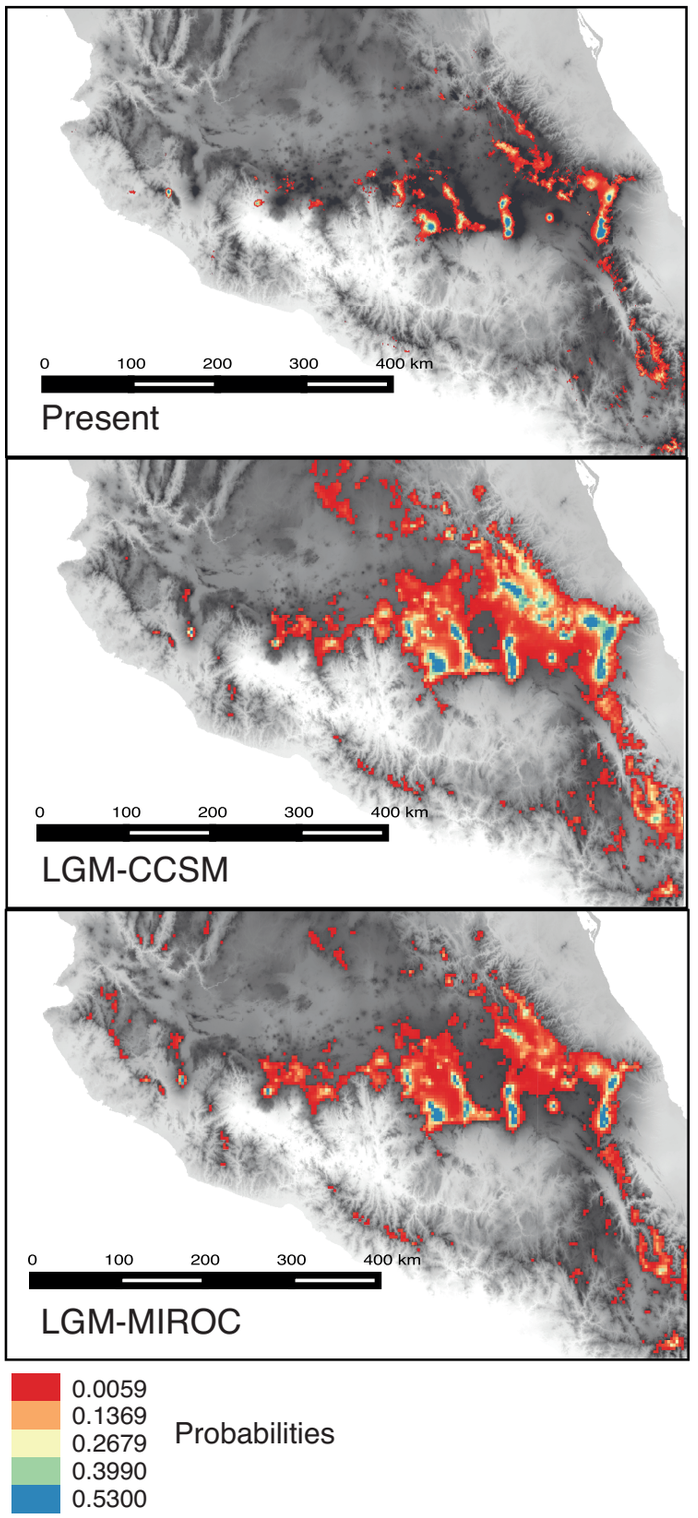

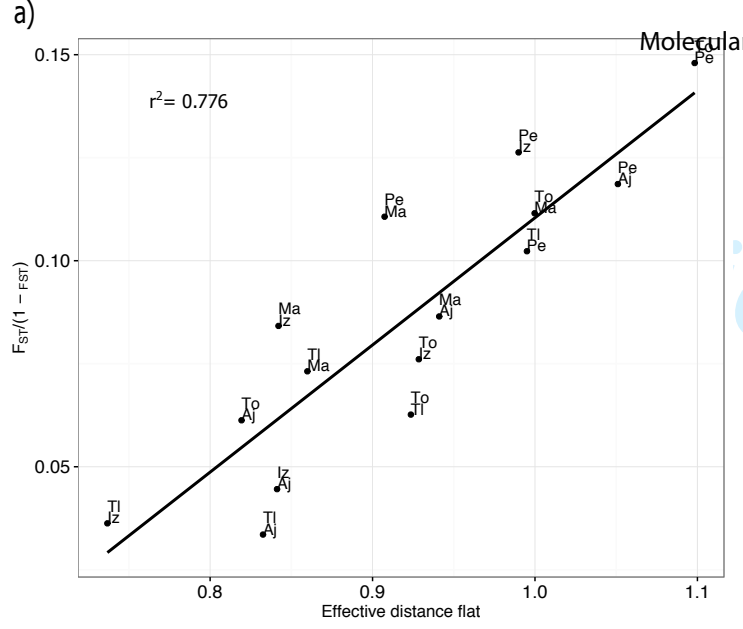
a)
r2= 0.776
FST/(1 − FST)
Effective distance flat
0.15
0.10
0.05
0.8
0.9
1.0
1.1
Pe
Pe
Pe
Pe
To
Ma
Tl
Pe
Ma
Ma
Aj
Ma
Iz
To
Tl
Ma
To
Aj
To
Tl
Iz
Aj
Tl
Iz
Tl
Aj

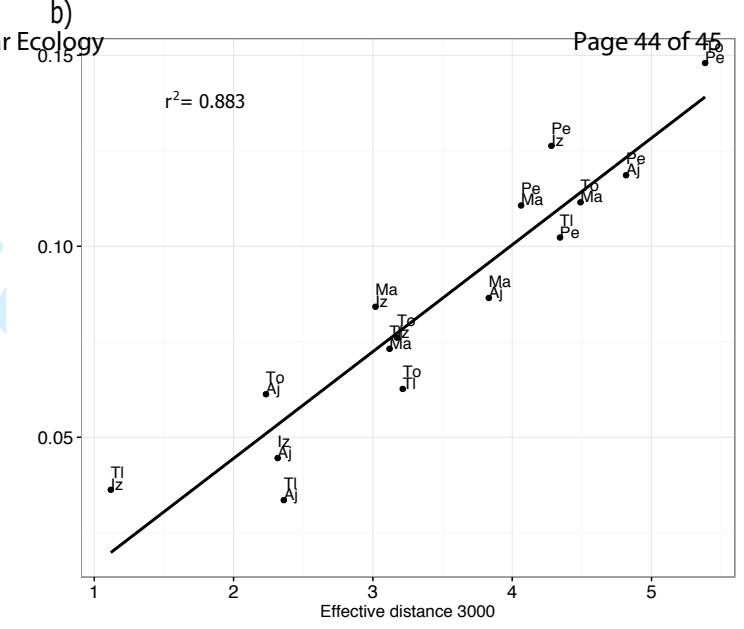
b)
r2= 0.883
Effective distance 3000
0.15
0.10
0.05
1
2
3
4
5
Pe
Pe
Pe
Pe
Pe
To
Ma
Tl
Pe
Ma
Iz
Ma
Aj
To
Iz
Ma
To
Aj
Tl
Iz
Aj
Tl
Aj

a)

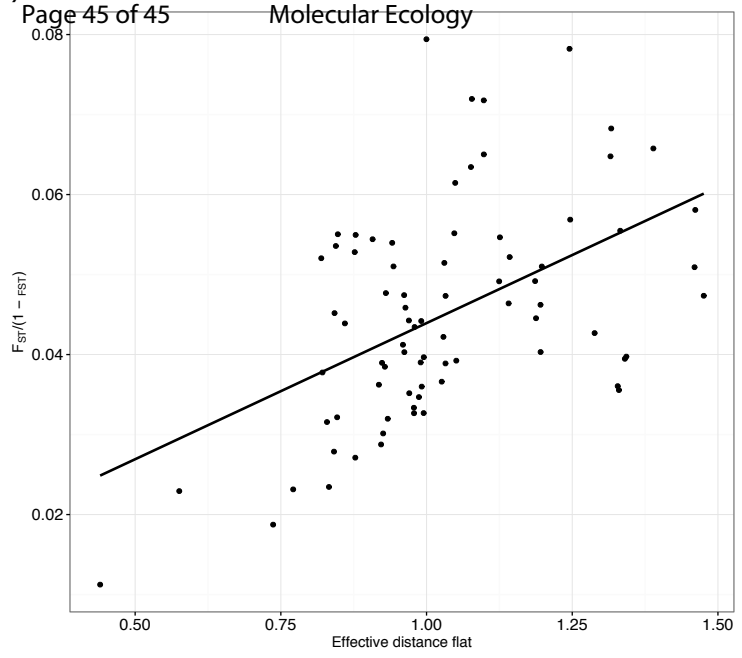
0.08
0.06
0.04
0.02
$F_{ST}/(1 - F_{ST})$
0.50
0.75
1.00
1.25
1.50
Effective distance flat

b)

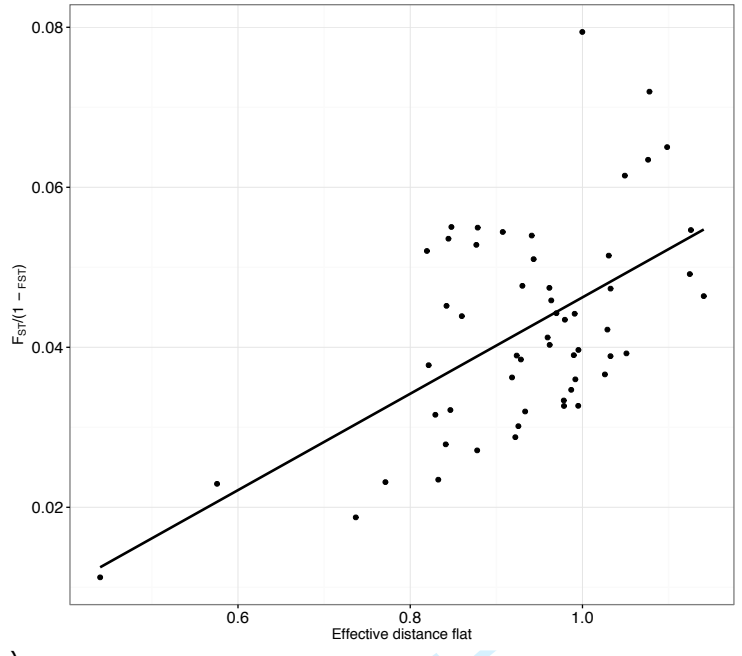
0.08
0.06
0.04
0.02
$F_{ST}/(1 - F_{ST})$
0.6
0.8
1.0
Effective distance flat

c)

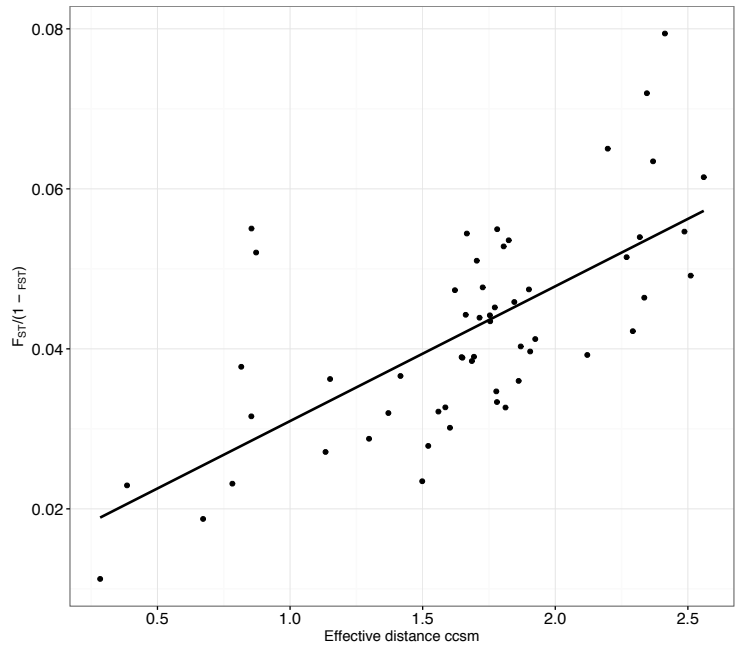
0.08
0.06
0.04
0.02
$F_{ST}/(1 - F_{ST})$
0.5
1.0
1.5
2.0
2.5
Effective distance ccsm